A Novel Full-Three-Dimensional MIMO Mobile-to-Mobile Channel Reference Model

Gholamreza Bakhshi
Department of Electrical and Computer Engineering
Yazd University, Yazd, Iran
Email: bakhshi@stu.yazduni.ac.ir

Kamal Shahtalebi
Department of Information Technology
University of Isfahan, Isfahan
Iran, Postal Code: 81746-73441
Email: shahtalebi@eng.ui.ac.ir

Hamidreza Saligheh Rad
Laboratory for Structural NMR Imaging
University of Pennsylvania, USA
Email: hsalig@mail.med.upenn.edu

***Abstract*—Analysis and design of multi-element antenna systems in mobile fading channels require a model for the space-time cross-correlation among the links of the underlying multiple-input multiple-output (MIMO) Mobile-to-Mobile (M-to-M) communication channel. In this paper, based on the Modified Geometrical Two-Ring (MGTR), a Full-Three-Dimensional (3-D) MIMO channel reference model for M-to-M communication systems is proposed. In the proposed method named the geometrical single-bounce two-sphere (SBTS) model, both transmitter and receiver are moving components. Assuming 3-D Non-isotropic and single-bounce scattering model, a closed-form expression for the space-time cross-correlation function (CCF) between each two sub channels is derived where includes many existing correlation models as special cases. Some simulation results are presented as special cases of the derived CCF.**

***Index Terms*—Mobile fading channels, mobile-to-mobile channels, MIMO channels, multi-element antenna systems, space-time correlation.**

I. Introduction

Mobile-to-Mobile communication channels are expected to play an important role in mobile ad-hoc networks (MANETs), intelligent transportation systems and relay-based cellular networks, where both the transmitter (Tx) and the receiver (Rx) are in motion. In opposition to the conventional Base-to-Mobile (B-to-M) cellular radio channels, in M-to-M channels, the base station (BS) is not stationary and therefore it is not free of local scattering.

In a typical macro-cell, the BS is elevated and receives the signal within a narrow beam-width, whereas the mobile station (MS) is surrounded by local scatterers. MIMO channel modelling of this typical macro-cell environment was investigated in [1] and [2]. However, in outdoor micro-cells, indoor picocells and the M-to-M communication channels, both Tx (BS/MS_T) and Rx (MS/MS_R) are normally surrounded by local scatterers. Clearly, the MIMO macro-cell models of [1] and [2] cannot be used for such environments. For these situations, we need a double-directional channel model (See e.g. [3]–[5], in which the double-directional concept is introduced and some measurements results are provided). Akki and Haber [6], [7] showed that the received envelope on M-to-M channels is Rayleigh faded under non line-of-sight (NLoS) condition, but the statistical properties differ from B-to-M channels. They proposed a reference model for Single-Input Single-Output (SISO) M-to-M Rayleigh fading channels. Methods for simulating SISO M-to-M channels have been proposed in [8] and [9]. Pätzold *et al.* proposed a theoretical reference model for narrow-band MIMO M-to-M communication channel [10]-[12]. This model is based on geometrical "Double-Bounce Two-Ring model" or in simplicity, geometrical "Two-Ring model" and belongs to the class of double-directional channel models. In [12] and [13] the realizable simulation models for MIMO M-to-M Channels are proposed that all of them are based on Two-Ring model. In [14], the authors have proposed the MGTR model for MIMO M-to-M communication channel. The MGTR model is based on the extension of geometrical "single-bounce two-ring" (SBTR) model proposed in [15] for MIMO B-to-M channel. The SBTR model belongs to the class of double-directional B-to-M channel models. In [15], the authors have avoided many difficulties of the two-ring model discussed in [16], [17]. Furthermore, the rightness of their model has been shown via real experimental data. The MGTR model, in comparison with SBTR, includes the mobility of both the transmitter and the receiver. A single- and double-bounced two-ring parametric reference model has been proposed in [18] for MIMO M-to-M Ricean fading channels and simulated.

All previously reported models assume that the field incident on the Tx or Rx antenna is composed of a number of waves travelling only in the horizontal plane. This assumption is acceptable only for certain environments, e.g., rural areas. However, it does not seem to be appropriate for urban environment in which the Tx and Rx antenna arrays are often located in close proximity to and lower than surrounding buildings. Scattered waves may propagate by diffraction from the tops of buildings down to the streets, and thus not necessarily travel horizontally [19]. In [19] a 3-D model,"Double-Bounce Two-Cylinder" model, is proposed for MIMO M-to-M Rayleigh fading channels and, in [20] the influence of this 3-D model on the Capacity of MIMO M-to-M Channels is investigated.

This paper proposes a full-3D theoretical reference model for MIMO M-to-M Rayleigh fading channels. This model is based on the MGTR model [14]. From the full-3D reference model, we derive a closed-form space-time correlation function (STCCF) for 3D Non-isotropic scattering environment.Furthermore, we present some simulation results to verify theoretical derivations.

978-1-4244-4474-8/09/$25.00 ©2009 IEEE

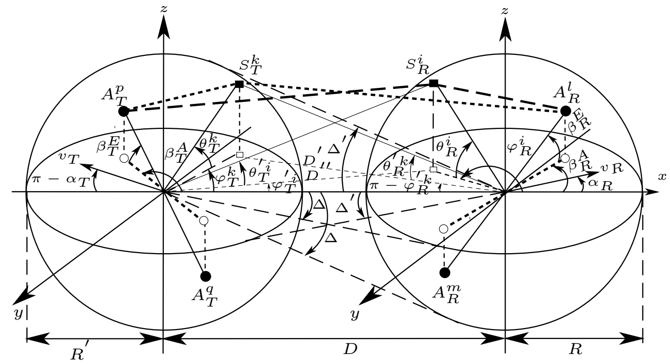

Fig. 1. The SBTS model for a 2×2 MIMO channel with 3-D distribution of scatterers around mobile transmitter MS_T (left) and mobile receiver MS_R (right).

The remainder of the paper is organized as follows. In section II we describe the SBTS, a 3-D theoretical reference model for MIMO M-to-M channels. Based on the SBTS model, in Section III a closed-form expression for the STCCF is derived. Section IV presents some simulation results to verify derived STCCF in III. Finally, concluding remarks are provided in Section V.

II. Theoretical reference model for MIMO M-to-M channels

Consider a narrow-band single-user MIMO communication system with n_T transmitter and n_R receiver antenna elements. Assume both Tx and Rx are in motion and equipped with low elevation antennas. The radio propagation environment is characterized by 3-D scattering with NLoS conditions between the transmitter and the receiver. The MIMO channel can be described by an $n_R \times n_T$ matrix $H(t) = [h_{ij}(t)]_{n_R \times n_T}$ of complex faded envelopes.

A. Geometrical SBTS model

The geometry of SBTS model is shown in figure 1 for a MIMO M-to-M channel with $n_T = n_R = 2$ antenna elements, where local scatterers of MS_T and MS_R are modelled to be distributed on two separate spheres. The key difference between our model and the other existing M-to-M models is that here only single-bounce rays are considered and multiple bounces are treated as secondary effects. This avoids the problem of double-bounce two-ring model. As it can be seen from figure 1, the local scatterers around the transmitter, denoted by S_T^k $(k = 1, 2, \ldots, N_T)$, are located on a sphere of radius R', while the local scatterers S_R^i $(i = 1, 2, \ldots, N_R)$ around the receiver lie on a separate sphere of radius R. The symbols φ_T and θ_T denote the main azimuth angle of departure (AAOD) and the main elevation angle of departure (EAOD), respectively and the symbols φ_R and θ_R denote the main azimuth angle of Arrival (AAOA) and the main elevation angle of arrival (EAOD),respectively. The symbols $\varphi_T^{'}$ and $\theta_T^{'}$ denote the auxiliary AAOD and the auxiliary EAOD, respectively and the symbols $\varphi_R^{'}$ and $\theta_R^{'}$ denote the auxiliary AAOA and the auxiliary EAOD,respectively. It is assumed that the radii R' and R are small in comparison with D, which is the distance between the transmitter and the receiver (i.e., $\{\max\{R, R'\} \ll D\}$). The antenna spacing at the transmitter and the receiver are denoted by δ_T and δ_R, respectively. Since the antenna spacing are generally small in comparison with the radii R' and R, we might assume that the inequality $\{\min\{R, R'\} \gg \max\{\delta_T, \delta_R\}\}$ is held. Angles β_T^A and β_R^A describe the orientation of the Tx and Rx antenna array in the x-y plane, respectively, relative to the x-axis. Similarly, angles β_T^E and β_R^E describe the elevation of the Tx's antenna array and Rx's antenna array relative to the x-y plane, respectively. Moreover, it is assumed that the Tx and the Rx move with speeds v_T and v_R and in the direction determined by the angle of motion α_T and α_R, respectively. Furthermore, 2Δ is the maximum angle spread at MS_T, determined by the 3-D scattering around MS_R in both azimuth and elevation direction. Similarly $2\Delta'$ is the maximum angle spread at MS_R, determined by the 3-D scattering around MS_T in both azimuth and elevation direction. From figure 1, it is clear that $\Delta = \arcsin(R/D)$, and $\Delta' = \arcsin(R'/D)$. Note that, geometry of our proposed model includes many existing geometrical models.

B. Derivation of the reference model

In this subsection, we derive the 3-D reference model for the MIMO M-to-M channel. In figure 1, by considering the forward channel (from MS_T to MS_R), the MS_R receives single-bounce rays from both the scatterer S_R^i around the MS_R and the scatterer S_T^k around the MS_T. For the frequency flat, sub-channel between the antenna elements A_T^p and A_R^l, $h_{lp}(t)$ denotes the time-varying complex baseband equivalent channel gain. Mathematical representation of the superposition of rays at the A_R^l, results in the following expression for the channel gain:

$$h_{lp}(t) = \sqrt{\frac{\eta_T}{N_T}} \sum_{k=1}^{N_T} \exp\{-j\frac{2\pi}{\lambda}(d_{A_T^p S_T^k} + d_{S_T^k A_R^l}) + j\Psi_T^k + j2\pi f_1^k t\} + \sqrt{\frac{\eta_R}{N_R}} \sum_{i=1}^{N_R} \exp\{ -j\frac{2\pi}{\lambda}(d_{A_T^p S_R^i} + d_{S_R^i A_R^l}) + j\Psi_R^i + j2\pi f_2^i t\} \quad (1)$$

where the first and the second summations correspond to the MS_T and MS_R spheres, respectively. This expression shows the role of AOAs and AODs in interrelation between the single-bounce two-sphere model in figure 1 and the $n_R \times n_T$ channel transfer matrix $H(t)$, in which $h_{lp}(t)$ is the element of row l and column p. The d_{XY} denotes the distance between X and Y, η_T and η_R show the respective contribution of scatterers around the MS_T and MS_R such that $\eta_T + \eta_R = 1$. N_T and N_R are the number of scatterers around the MS_T and MS_R, respectively. Ψ_T^k and Ψ_R^i are the associated phase shifts. λ is the wavelength and frequencies f_1^k and f_2^i are given by:

$$f_1^k = f_{T_{max}} \cos(\alpha_T - \varphi_T^k)\cos(\theta_T^k) + f_{R_{max}} \cos(\alpha_R - \varphi_R^{'k})\cos(\theta_R^{'k}) \quad (2)$$

$$f_2^i = f_{T_{max}} \cos(\alpha_T - \varphi_T^{'i})\cos(\theta_T^{'i}) + f_{R_{max}} \cos(\alpha_R - \varphi_R^{i})\cos(\theta_R^{i}) \quad (3)$$

where $f_{T_{max}} = v_T/\lambda$ and $f_{R_{max}} = v_R/\lambda$ are the maximum Doppler frequencies caused by the movement of the Tx and the Rx, respectively. We also assume $\left\{\Psi_T^k\right\}_{k=1}^{N_T}$ and $\left\{\Psi_R^i\right\}_{i=1}^{N_R}$ are mutually independent and identically distributed (i.i.d) random variables with uniform distributions over $[0, 2\pi)$.

In the next section we derive the space-time cross-correlation function (STCCF) of our SBTS reference model. In what follows, we call φ_T^k the AAoD, θ_T^K the EAOD, φ_R^i the AAOA, and θ_R^i the EAoA.

III. The STCCF of the Reference Model

The STCCF plays an important role in MIMO communication Channels. In this section we derive a closed-form expression for STCCF. The normalized space-time cross-correlation between two sub-channel gains $h_{lp}(t)$ and $h_{mq}(t)$ is defined by $\rho_{lp,mq}(\tau) = E\left[h_{lp}(t)h_{mq}^*(t+\tau)\right]$, where $(\cdot)^*$ and $E(\cdot)$ denote complex conjugate operation and the statistical expectation operation, respectively. Based on independent properties of Ψ_T^k and Ψ_R^i, it can be asymptotically written as:

$$\rho_{lp,mq}(\tau) = \lim_{N_T\to\infty} \frac{\eta_T}{N_T}\sum_{k=1}^{N_T} \exp\{-j\frac{2\pi}{\lambda}(d_{A_T^p S_T^k} - d_{A_T^q S_T^k} + d_{S_T^k A_R^l} - d_{S_T^k A_R^m}) - j2\pi f_1^k\tau\} + \lim_{N_R\to\infty} \frac{\eta_R}{N_R}\sum_{i=1}^{N_R} \exp\{-j\frac{2\pi}{\lambda}(d_{A_T^p S_R^i} - d_{A_T^q S_R^i} + d_{S_R^i A_R^l} - d_{S_R^i A_R^m}) - j2\pi f_2^i\tau\}. \quad (4)$$

For large values of N_T and N_R, the discrete AAODs, φ_T^k, EAODs, θ_T^k, AAOAs, φ_R^i, EAOAs, θ_R^i can be replaced with continuous random variables φ_T, θ_T, φ_R and θ_R with probability density function (pdf) $p(\varphi_T)$, $p(\theta_T)$, $p(\varphi_R)$ and $p(\theta_R)$, respectively. Therefore, (4) can be reduced to the following integral form:

$$\rho_{lp,mq}(\tau) = \eta_T \int_{\theta_T}\int_{\varphi_T} \exp\{-j\frac{2\pi}{\lambda}(d_{A_T^p S_T} - d_{A_T^q S_T} + d_{S_T A_R^l} - d_{S_T A_R^m}) - j2\pi f_1\tau\} p(\varphi_T)p(\theta_T)d\varphi_T d\theta_T + \eta_R \int_{\theta_R}\int_{\varphi_R} \exp\{-j\frac{2\pi}{\lambda}(d_{A_T^p S_R} - d_{A_T^q S_R} + d_{S_R A_R^l} - d_{S_R A_R^m}) - j2\pi f_2\tau\} p(\varphi_R)p(\theta_R)d\varphi_R d\theta_R \quad (5)$$

where f_1 and f_2 are the continues form of f_1^k and f_2^i in equations (2) and (3), respectively. All of the d_{XY}'s in first integral of equation (5) depend on φ_T and θ_T. Similarly, All of the d_{XY}'s in the second integral of equation (5) depend on φ_R and θ_R.

Using the law of cosines in appropriate triangles in figure 1, and assumption $\{\min\{R, R'\} \gg \max\{\delta_R, \delta_T\}\}$, we obtain the following approximations:

$$d_{A_T^p S_T} - d_{A_T^q S_T} \approx -\delta_T^{pq}\left[\sin\beta_T^E \sin\theta_T + \cos\beta_T^E \cos\theta_T \cos(\beta_T^A - \varphi_T)\right], \quad (6)$$

$$d_{S_T A_R^l} - d_{S_T A_R^m} \approx -\delta_R^{lm}\left[\sin\beta_R^E \sin\theta_R^{'} + \cos\beta_R^E \cos\theta_R^{'} \cos(\beta_R^A - \varphi_R^{'})\right] \quad (7)$$

$$d_{A_T^p S_R} - d_{A_T^q S_R} \approx -\delta_T^{pq}\left[\sin\beta_T^E \sin\theta_T^{'} + \cos\beta_T^E \cos\theta_T^{'} \cos(\beta_T^A - \varphi_T^{'})\right] \quad (8)$$

$$d_{S_R A_R^l} - d_{S_R A_R^m} \approx -\delta_R^{lm}\left[\sin\beta_R^E \sin\theta_R + \cos\beta_R^E \cos\theta_R \cos(\beta_R^A - \varphi_R)\right] \quad (9)$$

Now we apply the law of sines and we obtain the following identities:

$$\frac{D}{\sin(\varphi_R^{'} - \varphi_T)} = \frac{R'\cos\theta_T}{\sin(\pi - \varphi_R^{'})} \quad (10)$$

$$\frac{D^{'}}{\sin(\frac{\pi}{2} - \theta_R^{'})} = \frac{R'\sin\theta_T}{\sin\theta_R^{'}} \quad (11)$$

$$\frac{D}{\sin(\varphi_R - \varphi_T^{'})} = \frac{R\cos\theta_R}{\sin\varphi_T^{'}} \quad (12)$$

$$\frac{D^{''}}{\sin(\frac{\pi}{2} - \theta_T^{'})} = \frac{R\sin\theta_R}{\sin\theta_T^{'}} \quad (13)$$

From figure 1, $\max\{D'\} = D + R'$, $\min\{D'\} = D - R'$, $\max\{D''\} = D + R$ and, $\min\{D''\} = D - R$. Based on the assumption $\max\{R, R'\} \ll D$, we conclude that $\Delta \approx R/D$, $\Delta' \approx R'/D$, $D' \approx D$ and, $D'' \approx D$. This observation, together with $\sin\epsilon \approx \epsilon$ when ϵ is small, allows us to derive the following approximation from (10)-(13), respectively:

$$\varphi_R^{'} \approx \pi - \Delta'\sin\varphi_T\cos\theta_T \quad (14)$$

$$\theta_R^{'} \approx \Delta'\sin\theta_T \quad (15)$$

$$\varphi_T^{'} \approx \Delta\sin\varphi_R\cos\theta_R \quad (16)$$

$$\theta_T^{'} \approx \Delta\sin\theta_R \quad (17)$$

Furthermore, using $\sin\epsilon \approx \epsilon$ and $\cos\epsilon \approx 1$ when ϵ is small, together with (14)-(17), the following approximations are derived:

$$\cos(\beta_R^A - \varphi_R^{'}) \approx -\cos\beta_R^A + \Delta'\sin\beta_R^A\sin\varphi_T\cos\theta_T \quad (18)$$

$$\cos(\alpha_R - \varphi_R^{'}) \approx -\cos\alpha_R + \Delta'\sin\alpha_R\sin\varphi_T\cos\theta_T \quad (19)$$

$$\cos(\beta_T^A - \varphi_T^{'}) \approx \cos\beta_T^A + \Delta\sin\beta_T^A\sin\varphi_R\cos\theta_R \quad (20)$$

$$\cos(\alpha_T - \varphi_T^{'}) \approx \cos\alpha_T + \Delta\sin\alpha_T\sin\varphi_R\cos\theta_R \quad (21)$$

Now, by substituting (19) and (21) to continuous form of (2) and (3), respectively, the following approximations are derived:

$$f_1 \approx f_{T_{max}} \cos(\alpha_T - \varphi_T)\cos\theta_T - f_{R_{max}}\cos\alpha_R + f_{R_{max}}\Delta'\sin\alpha_R\sin\varphi_T\cos\theta_T \quad (22)$$

$$f_2 \approx f_{T_{max}}\cos\alpha_T + f_{T_{max}}\Delta\sin\alpha_T\sin\varphi_R\cos\theta_R + f_{R_{max}}\cos(\alpha_R - \varphi_R)\cos\theta_R \quad (23)$$

For any given $p(\varphi_T)$, $p(\varphi_R)$, $p(\theta_T)$ and $p(\theta_R)$ the right hand side (RHS) of equation (5) can be calculated numerically, using the trigonometric function relationships given in equations (6)-(9). Note that the RHS of equation (5) includes two parts. The first part corresponds to STCCF contributed by the scattering sphere around the MS_T, and the second part comes from the scattering sphere around the MS_R. Given the assumptions $\{\max\{R, R'\} \ll D\}$ and $\{\min\{R, R'\} \gg \max\{\delta_R, \delta_T\}\}$, and by plugging (6)-(9), (18) and (20) into (5), equation (5) can be approximate by:

$$\rho_{lp,mq}(\tau) \approx \eta_T \int_{\theta_T}\int_{\varphi_T} \exp\Bigg\{ j\frac{2\pi}{\lambda}\delta_T^{pq}\Big[\sin\beta_T^E\sin\theta_T + \cos\beta_T^E\cos\theta_T\cos(\beta_T^A - \varphi_T)\Big] + j\frac{2\pi}{\lambda}\Big[\delta_R^{lm}\Delta'\sin\beta_R^E\sin\theta_T - \delta_{R_x}^{lm} + \Delta'\delta_{R_y}^{lm}\sin\varphi_T\cos\theta_T\Big] - j2\pi f_1\tau\Bigg\} p(\varphi_T)p(\theta_T)d\varphi_T d\theta_T + \eta_R \int_{\theta_R}\int_{\varphi_R}\exp\Bigg\{ j\frac{2\pi}{\lambda}\Big[\delta_T^{pq}\Delta\sin\beta_T^E\sin\theta_R + \delta_{T_x}^{pq} + \Delta\delta_{T_y}^{pq} \times \sin\varphi_R\cos\theta_R\Big] + j\frac{2\pi}{\lambda}\delta_R^{lm}\Big[\sin\beta_R^E\sin\theta_R + \cos\beta_R^E\cos\theta_R \times \cos(\beta_R^A - \varphi_R)\Big] - j2\pi f_2\tau\Bigg\} p(\varphi_R)p(\theta_R)d\varphi_R d\theta_R \quad (24)$$

where $\delta_{T_x}^{pq} = \delta_T^{pq}\cos\beta_T^E\cos\beta_T^A$, $\delta_{T_y}^{pq} = \delta_T^{pq}\cos\beta_T^E\sin\beta_T^A$, $\delta_{R_x}^{lm} = \delta_R^{lm}\cos\beta_R^E\cos\beta_R^A$, and $\delta_{R_y}^{lm} = \delta_R^{lm}\cos\beta_R^E\sin\beta_R^A$.

Now we consider the 3-D non-isotropic scattering. Several different scatterer distributions, such as uniform, Gaussian, Laplacian, and von Mises, have been used in prior works to characterize the continuous random variables φ_T and φ_R. In this paper, we use the von Mises pdf because it approximates many of the previously mentioned distributions and leads to closed-form solutions for many useful situations [19]. The von Mises pdf is defined as [21]

$$p(\varphi) = \frac{1}{2\pi I_0(K)}\exp[K\cos(\varphi - \mu)] \quad (25)$$

where $\varphi \in [-\pi, \pi)$, $I_0(\cdot)$ is the zeroth-order modified Bessel function of the first kind, $\mu \in [-\pi, \pi)$ is the mean angle at which the scatterers are distributed in the $x - y$ plane, and k controls the spread of scatterers around the mean. To characterize the continuous random variables θ_T and θ_R, we use the pdf [22]

$$p(\theta) = \begin{cases} \frac{\pi}{4|\theta_m|}\cos\left(\frac{\pi}{2}\frac{\theta}{\theta_m}\right), & |\theta| \le |\theta_m| \le |\frac{\pi}{2}| \\ 0, & \text{otherwise} \end{cases}$$

where θ_m is the maximum elevation angle and takes values in the range $10^\circ \le |\theta_m| \le 20^\circ$ [23].

Now we consider the von Mises pdf for the Tx and Rx azimuth angles as $p(\varphi_T) = \exp[K_T\cos\varphi_T - \mu_T]/(2\pi I_0(K_T))$ and $p(\varphi_R) = \exp[K_R\cos\varphi_R - \mu_R]/(2\pi I_0(K_R))$, respectively, and by considering the pdf for the Tx and Rx elevation angles as $p(\theta_T) = \pi\cos(\pi\theta_T/(2\theta_{T_m}))/(4|\theta_{T_m}|)$ and $p(\theta_R) = \pi\cos(\pi\theta_R/(2\theta_{R_m}))/(4|\theta_{R_m}|)$ respectively. Under this conditions, and by plugging equations (22) and (23) to (24), calculating the φ.-dependent integrals by using the equality $\int_{-\pi}^{\pi}\exp(a\sin\varphi + b\cos\varphi)d\varphi = 2\pi I_0(\sqrt{a^2+b^2})$ [[24], eq. 3.338], the following expression for the STCCF is derived after some algebraic manipulations:

$$\rho_{lp,mq}(\tau) \approx \frac{\eta_T}{I_0(K_T)}\exp\left[-j\frac{2\pi}{\lambda}\delta_{R_x}^{lm} + j2\pi\tau f_{R_{max}}\cos\alpha_R\right] \int_{-\theta_{T_m}}^{\theta_{T_m}} \frac{\pi}{4|\theta_{T_m}|}\cos\left(\frac{\pi}{2}\frac{\theta_R}{\theta_{R_m}}\right) I_0\left(\sqrt{x^2+y^2}\cos\theta_T\right)\exp\left\{j\frac{2\pi}{\lambda}\ \zeta \sin\theta_T\right\}d\theta_T + \frac{\eta_R}{I_0(K_R)}\exp\left[j\frac{2\pi}{\lambda}\delta_{T_x}^{pq} - j2\pi\tau f_{T_{max}}\cos\alpha_T\right] \int_{-\theta_{R_m}}^{\theta_{R_m}} \frac{\pi}{4|\theta_{R_m}|}\cos\left(\frac{\pi}{2}\frac{\theta_R}{\theta_{R_m}}\right) I_0\left(\sqrt{z^2+w^2}\cos\theta_R\right)\exp\left\{j\frac{2\pi}{\lambda}\ \zeta \sin\theta_R\right\}d\theta_R \quad (26)$$

where $\zeta = \delta_T^{pq}\sin\beta_T^E + \delta_R^{lm}\sin\beta_R^E$, and parameters x, y, z and w are

$$x = j\frac{2\pi}{\lambda}\delta_{T_x}^{pq} - j2\pi\tau f_{T_{max}}\cos\alpha_T + K_T\cos\mu_T/\cos\theta_T,$$

$$y = j\frac{2\pi}{\lambda}(\delta_{T_y}^{pq} + \delta_{R_y}^{lm}\Delta') - j2\pi\tau(f_{T_{max}}\sin\alpha_T + \Delta' f_{R_{max}}\sin\alpha_R) + K_T\sin\mu_T/\cos\theta_T,$$

$$z = j\frac{2\pi}{\lambda}\delta_{R_x}^{lm} - j2\pi\tau f_{R_{max}}\cos\alpha_R + K_R\cos\mu_R/\cos\theta_R,$$

$$w = j\frac{2\pi}{\lambda}(\delta_{T_y}^{pq}\Delta + \delta_{R_y}^{lm}) - j2\pi\tau(\Delta f_{T_{max}}\sin\alpha_T + f_{R_{max}}\sin\alpha_R) + K_R\sin\mu_R/\cos\theta_R.$$

To obtain the STCCF for the 3-D MIMO M-to-M channel, the integrals in (26) have to be evaluated numerically, because they do not have closed-form solutions. Since θ_T and θ_R are small angles, i.e., $|\theta_T|, |\theta_R| \le 20^\circ$, using approximation $\cos\theta_T, \cos\theta_R \approx 1$, $\sin\theta_T \approx \theta_T$, and $\sin\theta_R \approx \theta_R$, solving the integrals in (26) leads to the following STCCF in a closed-form:

$$\rho_{lp,mq}(\tau) \approx \frac{\eta_T}{I_0(K_T)}\exp\left[-j\frac{2\pi}{\lambda}\delta_{R_x}^{lm} + j2\pi\tau f_{R_{max}}\cos\alpha_R\right] I_0\left(\sqrt{x_1^2+y_1^2}\right)\frac{\cos\left(\frac{2\pi}{\lambda}\ \zeta\ \theta_{T_m}\right)}{\left[1 - \left(\frac{4\ \zeta\ \theta_{T_m}}{\lambda}\right)^2\right]} + \frac{\eta_R}{I_0(K_R)}\exp\left[j\frac{2\pi}{\lambda}\delta_{T_x}^{pq} - j2\pi\tau f_{T_{max}}\cos\alpha_T\right] I_0\left(\sqrt{z_1^2+w_1^2}\right)\frac{\cos\left(\frac{2\pi}{\lambda}\ \zeta\ \theta_{R_m}\right)}{\left[1 - \left(\frac{4\ \zeta\ \theta_{R_m}}{\lambda}\right)^2\right]} \quad (27)$$

where the parameters x_1, y_1, z_1 and w_1 are

$$x_1 = j\frac{2\pi}{\lambda}\delta_{T_x}^{pq} - j2\pi\tau f_{T_{max}}\cos\alpha_T + K_T\cos\mu_T,$$

$$y_1 = j\frac{2\pi}{\lambda}(\delta_{T_y}^{pq} + \delta_{R_y}^{lm}\Delta') - j2\pi\tau(f_{T_{max}}\sin\alpha_T + \Delta' f_{R_{max}}\sin\alpha_R) + K_T\sin\mu_T,$$

$$z_1 = j\frac{2\pi}{\lambda}\delta_{R_x}^{lm} - j2\pi\tau f_{R_{max}}\cos\alpha_R + K_R\cos\mu_R,$$

$$w_1 = j\frac{2\pi}{\lambda}(\delta_{T_y}^{pq}\Delta + \delta_{R_y}^{lm}) - j2\pi\tau(\Delta f_{T_{max}}\sin\alpha_T + f_{R_{max}}\sin\alpha_R) + K_R\sin\mu_R.$$

Note that, many existing correlation functions are special cases of our 3-D MIMO M-to-M space-time correlation function in (27). For example:

- For 2-D distribution of scatterers ($\theta_{T_m} = \theta_{R_m} = 0$), our reference model reduces to 2-D MIMO M-to-M communication, or same MGTR model [14]. In this conditions, the STCCF in (27) simplifies to equation (22) of [14], by substituting $K_T = K_R = 0$ in (27) for 2-D isotropic scattering (in azimuth plane) around the MS_T and the MS_R.
- For 2-D distribution of scatterers ($\theta_{T_m} = \theta_{R_m} = 0$), and stationary MS_T ($f_{T_{max}} = 0$) our 3-D reference model's STCCF reduces to MIMO B-to-M communication channel model, SBTR model, proposed in [15] (eq. (7) of [15]).
- For 2-D distribution of scatterers ($\theta_{T_m} = \theta_{R_m} = 0$), stationary MS_T ($f_{T_{max}} = 0$), and no scattering around the MS_T as in a macro-cell ($\eta_T = 0$), our 3-D reference model's STCCF reduces to MIMO B-to-M communication channel model proposed in [2].
- If all of the above items's assumptions are established, and $l = m$ and $p = q$, our reference model's STCCF simplifies to conventional "One-Ring" model for SISO B-to-M communication channel. This reduces (27) to the simplest special case, well-known Clark's temporal correlation function, i.e., $J_0(2\pi f_{R_{max}}\tau)$ [25], where $J_0(\cdot)$ is the Bessel function of the first kind of zero order.

IV. Simulation Results

In this section, we present some simulation results to verify the theoretical STCCF of the proposed reference model. The following parameters were chosen for the model. The angles of antenna array at transmitter β_T^A and β_T^E, and at the receiver β_R^A and β_R^E were defined as $\beta_T^A = \pi/4$, $\beta_T^E = \pi/3$, $\beta_R^A = \pi/4$ and $\beta_R^E = \pi/2$. At the transmitter side, the angle of motion α_T was set to $\pi/4$, while the receiver was moving at an angle of $\alpha_R = 0$. Identical maximum Doppler frequencies $f_{T_{max}} = f_{R_{max}} = 91$ Hz was assumed, and the wavelength λ was set to $\lambda = 0.15$ m. Furthermore, the parameters Δ, Δ' and η_R have set to $\Delta = \pi/3$, $\Delta' = \pi/6$ and $\eta_R = 0.2$, according to table I of [15]. Maximum elevation angle at Tx and Rx was $\theta_{T_m} = \theta_{R_m} = 20°$. The temporal auto-correlation function

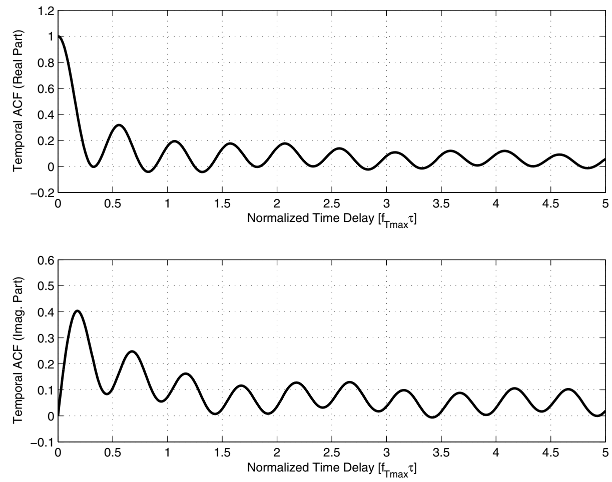

Fig. 2. Temporal ACF of the proposed reference model ($\delta_T^{pq} = \delta_R^{lm} = 0$).

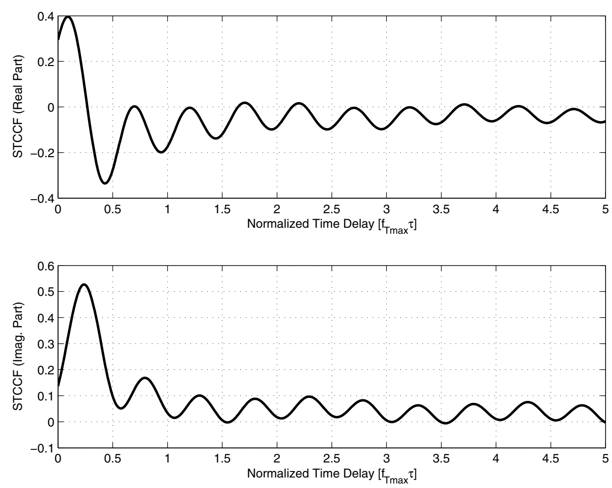

Fig. 3. The STCCF of the proposed reference model for $\delta_T^{pq} = \delta_R^{lm} = 0.5\lambda$.

(ACF) is illustrated in figure 2. Figure 3 shows the space-time correlation function of the proposed reference model for $\delta_T^{pq} = \delta_R^{lm} = 0.5\lambda$.

The 2-D space-time correlation functions for M-to-M channels proposed in [10]- [14] and [18] suggest that two vertically placed antennas are completely correlated and no diversity gain is available [19]. However, the proposed 3-D space-time correlation function shows that vertically placed antennas can have small correlations and provide considerable diversity gain. To illustrate this, figure 4 shows the space-time correlation functions of two vertically spaced antennas at the Tx for several maximum elevation angles θ_{T_m}. Other parameters used to obtain curves in figure 4 are $n_R = 1$ and $\beta_T^E = \pi/2$. As the maximum elevation angle θ_{T_m} increases from 0° to 20°, the correlation between the two antennas reduces dramatically.

V. Conclusion

This paper proposed a theoretical 3-D reference model for Rayleigh fading MIMO M-to-M channels. This 3-D reference

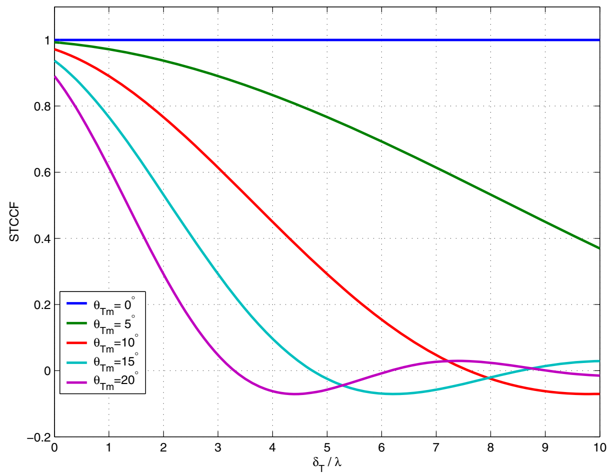

Fig. 4. The normalized STCCF of two vertically spaced antennas at the Tx for several maximum elevation angles θ_{T_m}.

model was based on extension (from 2-D to 3-D) of modified geometrical two-ring model, that avoids the technical difficulties of the two-ring model. The closed-form cross-correlation function for 3-D non-isotropic scattering was derived for this proposed reference model. It is shown that many existing correlation functions are special cases of our 3-D MIMO M-to-M space-time correlation function. Finally, some simulation results are presented to verify theoretical derivations.

REFERENCES

[1] D-S. Shiu,G. J. Foschini, M. J. Gans, and J. M. Kahn. "Fading correlation and its effect on the capacity of multielement antenna systems," *IEEE Transactions on Communications*, vol. 48, No. 3, pp. 502-513, March 2000.

[2] A. Abdi and M. Kaveh, "A space-time correlation model for multielement antenna systems in mobile fading channels," *IEEE J. Select. Areas Commun.*, vol. 20, pp. 550-560, Apr. 2002.

[3] M. Steinbauer, D. Hampicke, G. Sommerkorn, A. Schneider, A. F. Molisch, R. Thoma, and E. Bonek, "Array measurement of the double-directional mobile radio channel," in *Proc. IEEE Veh. Technol. Conf.*, pp. 1656-1662, Tokyo, Japan, 2000.

[4] M. Steinbauer, A. F. Molisch, and E. Bonek, "The double-directional radio channel," *IEEE Antennas Propagat. Mag.*, vol. 43, pp. 51-63, Aug. 2001.

[5] D. Gesbert, H. Bolcskei, D. A. Gore, and A. J. Paulraj, "Outdoor MIMO wireless channels: models and performance prediction," *IEEE Trans. on Commun.*, vol. 50, pp. 1926-1934, Dec. 2002.

[6] A. S. Akki, F. Haber, "A statistical model of radio mobile-to-mobile land communication channel", *IEEE Trans. on Veh. Technology*, vol. 35, pp.2-10, Feb. 1986.

[7] A. S. Akki, "Statistical properties of mobile-to-mobile land communication channels", *IEEE Trans. on Veh. Technology*, vol.43, pp.826-831. Nov. 1994.

[8] C. S. Patel, G. L. Stüber, and T. G. Pratt, "Simulation of Rayleigh-faded mobile-to-mobile communication channels," *IEEE Trans. on Commun.*, vol. 53, pp. 1876-1884, November 2005.

[9] A. G. Zajić and G. L. Stüber, "A new simulation model for mobile-to-mobile Rayleigh fading channels," *Proc. IEEE WCNC 06*, vol. 3, pp. 1266-1270, Las Vegas, NV, USA, April 2006.

[10] M. Pätzold, B. O. Hogstad, N. Youssef, and D. Kim, "A MIMO mobile-to-mobile channel model: Part I-the reference model", *Proc. IEEE PIMRC 05*, pp. 573- 578, Berlin, Germany, September 2005.

[11] B. O. Hogstad, M. Pätzold, N. Youssef, and D. Kim, "A MIMO mobile-to-mobile channel model: Part II-the simulation model", *Proc. IEEE PIMRC 05*, pp. 562-567, Berlin, Germany, September 2005.

[12] M. Pätzold,B. O. Hogstad and N. Youssef, "Modeling, analysis, and simulation of MIMO mobile-to-mobile fading channels", *IEEE Trans. Wireless Comm.* , vol. 7, pp. 510520, 2008.

[13] A. G. Zajić and G. L. Stüber, "Simulation Models for MIMO Mobile-to-Mobile Channels", in *Proc. IEEE MILCOM'06*, pp. 1-7, Washington, D.C., USA, Oct. 2006.

[14] G. Bakhshi, R. Saadat, K. Shahtalebi, "A Modified Two-Ring Reference Model for MIMO Mobile-to-Mobile Communication Channels," *Proc. of International Symposium on Telecommunication (IST'08)*, Tehran, Iran, September 2008.

[15] S. Wang, A. Abdi, J. Salo, H. M. El-Sallabi, J. W. Wallace, P. Vainikainen, M. A. Jensen, "Time-Varying MIMO Channels: Parametric Statistical Modeling and Experimental Results", *IEEE Trans. on Veh. Technology*, vol. 56, pp. 1949-1963, July 2007.

[16] K. Yu and B. Ottersten, "Models for MIMO propagation channels: A review", *Wirel. Commun. Mob. Comput.*, vol. 2, pp. 653-666, 2002.

[17] K. Yu, "*Multiple-Input Multiple-Output Radio Propagation Channels: Characteristics and Models*", Doctoral thesis, Signals, Sensors and Systems, Royal Institute of Technology (KTH), 2005.

[18] A. G. Zajić and G. L. Stüber, "Space-Time Correlated Mobile-to-Mobile channels: Modelling and Simulation," *IEEE Trans. Vehicular Techn.*, vol. 57, No. 2, pp. 715726, 2008.

[19] A. G. Zajić and G. L. Stüber, "A three-dimensional MIMO mobile-to-mobile channel model," in *Proc. IEEE WCNC'07*, pp. 1883-1887, Hong Kong, March 2007.

[20] A. G. Zajić and G. L. Stüber, "Influence of 3-D Spatial Correlation on the Capacity of MIMO Mobile-to-Mobile Channels," in *Proc. IEEE VTC2007-Spring*, pp. 461-465, Dublin, April 2007.

[21] A. Abdi, J.A. Barger, and M. Kaveh, "A parametric model for the distribution of the angle of arrival and the associated correlation function and power spectrum at the mobile station," *IEEE Trans. on Veh. Tech.*, vol. 51, pp. 425434, May 2002.

[22] J.D. Parsons and A.M.D. Turkmani, "Characterisation of mobile radio signals: model description," *IEE Proc. I, Commun., Speach, and Vision*, vol. 138, pp. 549556, Dec. 1991.

[23] Y. Yamada, Y. Ebine, and N. Nakajima, "Base station/vehicular antenna design techniques employed in high capacity land mobile communications system," *Rev. Elec. Commun. Lab.*, NTT, pp. 115121, 1987.

[24] I. S. Gradshteyn and I. M. Rizhik, *Table of Integral, Series and Products*, 5th ed., A. Jeffrey, Ed., San Diego, CA: Academic, 1994.

[25] R. H. Clarke, "A statistical theory of mobile-radio reception," *Bell Syst. Tech. J.*, vol. 47, pp. 957-1000, July-August 1968.